

Differential Regulation of Protrusion and Polarity by PI(3)K during Neutrophil Motility in Live Zebrafish

Sa Kan Yoo,¹ Qing Deng,² Peter J. Cavnar,² Yi I. Wu,³ Klaus M. Hahn,³ and Anna Huttenlocher^{2,*}

¹Program in Cellular and Molecular Biology

²Departments of Pediatrics and Medical Microbiology and Immunology, 4205 Microbial Sciences Building, 1550 Linden Drive University of Wisconsin-Madison, Madison, WI 53706, USA

³Department of Pharmacology and Lineberger Cancer Center, University of North Carolina, Chapel Hill, NC 27599, USA

*Correspondence: huttenlocher@wisc.edu

DOI 10.1016/j.devcel.2009.11.015

SUMMARY

Cell polarity is crucial for directed migration. Here we show that phosphoinositide 3-kinase (PI(3)K) mediates neutrophil migration *in vivo* by differentially regulating cell protrusion and polarity. The dynamics of PI(3)K products PI(3,4,5)P₃-PI(3,4)P₂ during neutrophil migration were visualized in living zebrafish, revealing that PI(3)K activation at the leading edge is critical for neutrophil motility in intact tissues. A genetically encoded photoactivatable Rac was used to demonstrate that localized activation of Rac is sufficient to direct migration with precise temporal and spatial control *in vivo*. Similar stimulation of PI(3)K-inhibited cells did not direct migration. Localized Rac activation rescued membrane protrusion but not anteroposterior polarization of F-actin dynamics of PI(3)K-inhibited cells. Uncoupling Rac-mediated protrusion and polarization suggests a paradigm of two-tiered PI(3)K-mediated regulation of cell motility. This work provides new insight into how cell signaling at the front and back of the cell is coordinated during polarized cell migration in intact tissues within a multicellular organism.

INTRODUCTION

Cell polarization is necessary for the migration of cells in diverse processes including embryogenesis, inflammation, and tumor metastasis. Our current understanding of morphologic polarity during cell migration is derived primarily from chemotaxis studies using *Dictyostelium discoideum* and isolated mammalian cells, such as neutrophils, *in vitro* (Devreotes and Janetopoulos, 2003; Insall and Machesky, 2009; Janetopoulos and Firtel, 2008; Kay et al., 2008; Rericha and Parent, 2008; Stephens et al., 2008; Van Haastert and Veltman, 2007). While the molecular events that regulate the dynamics of the cell's leading edge or rear have been the focus of numerous studies, the principle that defines cell polarity between the front and the back is poorly understood. In addition, little is known about how polarized cell migration is regulated in three-dimensional (3D) tissue environments *in vivo* because few systems are amenable to high resolu-

tion imaging of the spatiotemporal dynamics of signaling in live cells within multicellular organisms. Experiments performed *in vivo* and using 3D conditions have sometimes yielded results that are contradictory to those observed using two-dimensional (2D) surfaces (Cukierman et al., 2001; Lammermann et al., 2008). For example, migration of dendritic cells in the interstitial tissues does not require integrins, which are indispensable adhesion proteins for motility over 2D surfaces (Lammermann et al., 2008). Thus, development of a system to study cell signaling and polarity during cell migration in physiological settings is critical for increasing our understanding of what is occurring *in vivo*.

Type I phosphoinositide 3-kinases (PI(3)Ks) generate the intracellular second messengers phosphatidylinositol (3,4,5)P₃-phosphatidylinositol(3,4)P₂ (PI(3,4,5)P₃-PI(3,4)P₂), which are critical regulators of a wide variety of cellular processes including cell migration (Barberis and Hirsch, 2008; Hawkins and Stephens, 2007; Vanhaesebroeck et al., 2005). PI(3)K regulates forward protrusion of the leading edge by activating Rac through a Rac GEF, such as DOCK (Nishikimi et al., 2009). PI(3)K was originally considered a central regulator of gradient sensing during chemotaxis of *D. discoideum* and isolated neutrophils (Hirsch et al., 2000; Li et al., 2000; Niggli and Keller, 1997; Parent et al., 1998; Sasaki et al., 2000; Servant et al., 2000), but a series of recent *in vitro* studies have eroded this view (Andrew and Insall, 2007; Chen et al., 2007; Ferguson et al., 2007; Heit et al., 2008; Hoeller and Kay, 2007; Nishio et al., 2007). These recent studies have suggested that PI(3)K is dispensable for eukaryotic chemotaxis and has only context-dependent roles in 2D environments. For example, in the presence of specific chemoattractants and/or in shallow gradients of chemoattractants, chemotaxis does not require PI(3)K activity (Andrew and Insall, 2007; Ferguson et al., 2007; Heit et al., 2008; Hoeller and Kay, 2007; Nishio et al., 2007). Therefore, the models that place PI(3)K as an indispensable compass that regulates gradient sensing during chemotaxis are no longer widely accepted (Insall and Machesky, 2009; Janetopoulos and Firtel, 2008; Kay et al., 2008; Rericha and Parent, 2008; Stephens et al., 2008; Van Haastert and Veltman, 2007). Although there are several studies that suggest that PI(3)K regulates interstitial migration of leukocytes *in vivo* (Hirsch et al., 2000; Li et al., 2000; Nombela-Arrieta et al., 2004; Sasaki et al., 2000), this view also needs to be re-evaluated based on the recent *in vivo* findings that suggest that PI(3)K regulates leukocyte emigration from the blood vessel rather than interstitial migration (Liu et al., 2007; Stephens et al.,

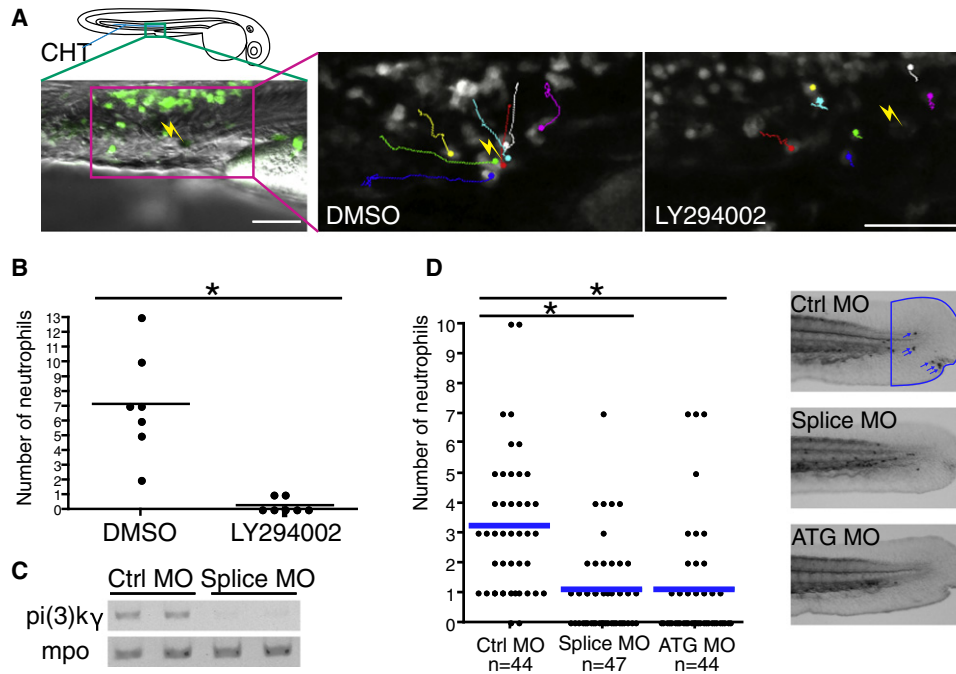


Figure 1. PI(3)K γ Is Necessary for Directed Migration of Neutrophils In Vivo

(A) Sixty-five micromolar LY294002 treatment inhibits attraction of neutrophils to a laser wound in the caudal hematopoietic tissue (CHT). The lines indicate tracking of individual neutrophils over 30 min and the yellow thunder shows the position of the laser wound. Note that neutrophils migrate rapidly toward the wound in control (DMSO), but not after LY294002 treatment (Movie S1). Scale bar = 50 μ m.

(B) The number of neutrophils that reach the laser wound in the CHT within 30 min is quantified (seven movies for each condition, * $p < 0.001$, two-tailed unpaired t test). Note that LY294002 treatment inhibits attraction of neutrophils to the wound.

(C) Splice morpholino disturbs splicing of pi(3)k γ transcript. Mpo transcript indicates integrity of neutrophils in morphants.

(D) Knockdown of PI(3)K γ inhibits directional migration of neutrophils to wounds (neutrophils are indicated with blue arrows in control, * $p < 0.001$, two-tailed unpaired t test). Data of (D) are representative of three separate experiments.

2008). In addition, live imaging-based studies have shown that PI(3)K products PI(3,4,5)P₃-PI(3,4)P₂ are not polarized during directional migration of primordial germ cells and endodermal cells in zebrafish (Dumstrei et al., 2004; Mizoguchi et al., 2008), raising further questions about the importance of polarized PI(3)K signaling during chemotaxis in vivo.

To study how PI(3)K activity regulates neutrophil motility in vivo, we used zebrafish embryos, which have been an emerging tool for the study of immune responses (Mathias et al., 2006; Niethammer et al., 2009; Trede et al., 2004). Here we demonstrate a novel two-tiered PI(3)K-mediated regulation of cell motility through both the modulation of Rac-mediated protrusion at the leading edge and anteroposterior polarity of F-actin dynamics.

RESULTS

PI(3)K γ Is Necessary for Directed Migration of Neutrophils In Vivo

To determine how PI(3)K regulates directed migration in vivo independent of its effects on extravasation, we developed a novel wound-induced chemotaxis system based on live imaging using the transgenic line *Tg(MPO:GFP)^{uw}*, in which neutrophils stably express GFP (Mathias et al., 2006). Autofluorescent pigment cells were laser-wounded in the caudal hematopoietic tissue (CHT), where neutrophils accumulate in zebrafish larvae at 2–3 days post fertilization (dpf) (Murayama et al.,

2006). The position of CHT was selected to exclude effects of PI(3)K inhibition on extravasation (Liu et al., 2007). Neutrophils in the CHT are relatively immotile at rest compared to neutrophils in the mesenchymal tissues of the head (see Movie S1 available online). The laser wounding induced rapid recruitment of neutrophils in controls (average 7 neutrophils in 30 min, $n = 7$). However, neutrophil recruitment to the wound was dramatically inhibited ($n = 7$) with the standard PI(3)K inhibitor LY294002 applied at 65 μ M, a concentration comparable to what has been used both in vitro and in vivo in previous studies (Andrew and Insall, 2007; Grabher et al., 2007; Sasaki et al., 2000; Servant et al., 2000) (Figures 1A and 1B; Movie S1). We also confirmed that LY294002 inhibits neutrophil recruitment to the wound in a dose-dependent manner by performing Sudan Black staining of embryos whose tail fins were mechanically wounded by a needle (Figure S1A). PI(3)K γ , class 1B p110 γ , is the isoform which is considered to be involved in chemotaxis of mammalian neutrophils (Barberis and Hirsch, 2008; Hawkins and Stephens, 2007; Vanhaesebroeck et al., 2005). Consistent with this, the PI(3)K γ -specific inhibitor AS-605240 (Camps et al., 2005) inhibited neutrophil attraction to wounds (Figure S1B). Further, we employed a genetic approach to knockdown PI(3)K γ (*zgc:77033*) using two different morpholino antisense oligos which disturb splicing and translation separately (Figure 1C). These morpholinos did not have any obvious effects on the location or number of neutrophils (Figure S1C). However, depletion of PI(3)K γ in

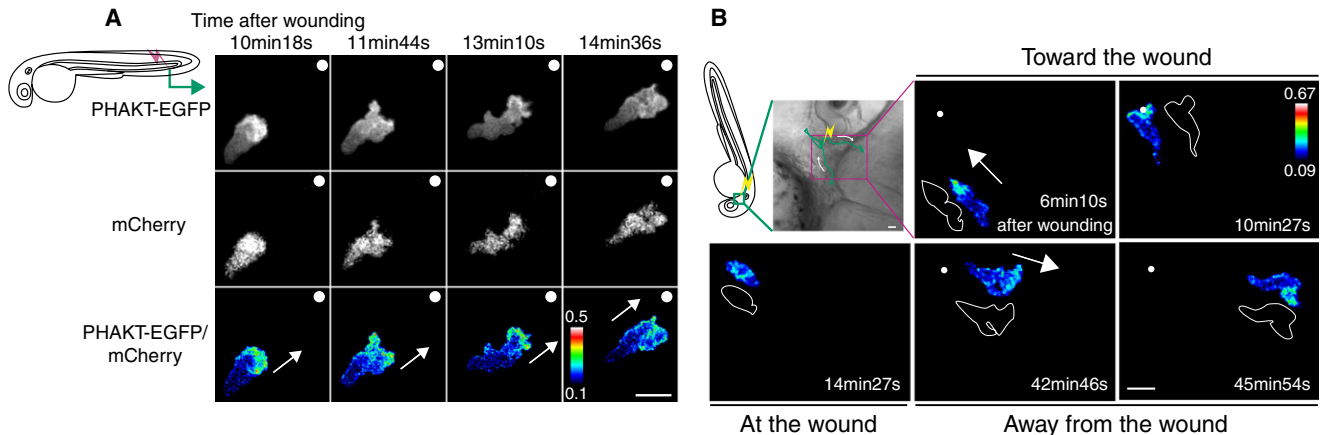


Figure 2. PHAKT-EGFP Translocates to the Leading Edge When Neutrophils Come To and Leave Laser-Induced Wounds

(A) Time-lapse ratiometric imaging (PHAKT-EGFP/mCherry) reveals $\text{PI}(3,4,5)\text{P}_3\text{-PI}(3,4)\text{P}_2$ localization at the leading edge during attraction to a laser wound in the tail fin (Movie S2A). The white dots and arrows indicate the position of the wound and direction of migration respectively. Scale bar = 10 μm .

(B) Reversal of $\text{PI}(3,4,5)\text{P}_3\text{-PI}(3,4)\text{P}_2$ (ratiometric imaging of PHAKT-EGFP/mCherry) when a neutrophil leaves the laser wound (Movie S2B). Note loss of $\text{PI}(3,4,5)\text{P}_3\text{-PI}(3,4)\text{P}_2$ polarity at the wound, followed by reversal of polarity to the opposite pole away from the wound when the neutrophil leaves the wound (green line, tracking of a neutrophil; yellow thunder, position of the laser wound; white arrows, direction of migration; illustration with white line, morphology of a neutrophil). Data are representative of more than five time-lapse movies from a minimum of three separate experiments. The numerical values of ratiometric analysis are shown in the scales. Scale bar = 10 μm .

zebrafish larvae significantly impaired neutrophil attraction to wounds (Figure 1D), indicating that $\text{PI}(3)\text{K}\gamma$ is required for directional migration of neutrophils in vivo.

Live Imaging of $\text{PI}(3,4,5)\text{P}_3\text{-PI}(3,4)\text{P}_2$ during Neutrophil Directed Migration In Vivo

Numerous studies using in vitro systems have reported that $\text{PI}(3,4,5)\text{P}_3\text{-PI}(3,4)\text{P}_2$ is localized to the leading edge of *D. discoideum* and neutrophils in vitro (Parent et al., 1998; Servant et al., 2000); however, it has not been possible to investigate spatio-temporal dynamics of $\text{PI}(3)\text{K}$ activity in neutrophils migrating rapidly in vivo. In addition, zebrafish primordial germ cells or endodermal cells perform chemotaxis to SDF1 without asymmetric polarization of $\text{PI}(3,4,5)\text{P}_3\text{-PI}(3,4)\text{P}_2$ (Dumstrei et al., 2004; Mizoguchi et al., 2008). Therefore we established in vivo high-resolution ratiometric imaging analysis in zebrafish to detect $\text{PI}(3)\text{K}$ products $\text{PI}(3,4,5)\text{P}_3\text{-PI}(3,4)\text{P}_2$ using modifications of previously reported methods for fibroblasts and dendritic cells in vitro (Arrieumerlou and Meyer, 2005). In vivo ratiometric imaging excludes the pseudosignals caused by volume effects of the cytoplasm or the cell membrane, which can be especially problematic in 3D environments. To visualize dynamics of $\text{PI}(3,4,5)\text{P}_3\text{-PI}(3,4)\text{P}_2$ in vivo, we expressed a probe for $\text{PI}(3,4,5)\text{P}_3\text{-PI}(3,4)\text{P}_2$ (PH domain of AKT fused to EGFP) and mCherry (a cytoplasmic volume marker) specifically in neutrophils by using the MPO promoter. Ratiometric imaging revealed that neutrophils generate $\text{PI}(3,4,5)\text{P}_3\text{-PI}(3,4)\text{P}_2$ at the leading edge pseudopods when neutrophils migrate to a laser-induced wound (Figure 2A; Movie S2A). We found that the leading edge pseudopod bifurcates after formation and that one of the bifurcated pseudopods becomes dominant in the direction of motility while $\text{PI}(3,4,5)\text{P}_3\text{-PI}(3,4)\text{P}_2$ remains at dominant pseudopods and is lost from retracted pseudopods (Figure 2A; Movie S2A). This migration mode is consistent with the motility model suggested recently based on the analysis of *D. discoideum* in

shallow gradients and also reported in zebrafish leukocytes (Andrew and Insall, 2007; Cvejic et al., 2008). In control studies, we confirmed that ratiometric imaging of EGFP/mCherry does not show any polarized signal (Figure S2A).

Previously, we reported that neutrophils migrate away from a wound after reaching the wound in zebrafish using highly directional migration, and suggested that reverse migration may contribute to resolution of inflammation (Mathias et al., 2006). To determine if polarized dynamics of $\text{PI}(3,4,5)\text{P}_3\text{-PI}(3,4)\text{P}_2$ are also observed in neutrophils during reverse migration, we performed ratiometric imaging of PHAKT-EGFP/mCherry during neutrophil bidirectional trafficking induced by wounding. Ratiometric imaging revealed that neutrophils lose polarity of $\text{PI}(3,4,5)\text{P}_3\text{-PI}(3,4)\text{P}_2$ at the laser-induced wound, and during reverse migration from the wound repolarize $\text{PI}(3,4,5)\text{P}_3\text{-PI}(3,4)\text{P}_2$ to the opposite pole away from the wound (Figure 2B; Movie S2B). We also observed dynamic reversal of $\text{PI}(3,4,5)\text{P}_3\text{-PI}(3,4)\text{P}_2$ at a mechanically induced wound in the tail fin when neutrophils leave the wound (Figure S2B and Movie S2C). Thus, although the regulatory mechanisms that mediate reverse migration remain elusive, polarity of $\text{PI}(3,4,5)\text{P}_3\text{-PI}(3,4)\text{P}_2$ is reversed when neutrophils leave the wound after attraction, suggesting that $\text{PI}(3)\text{K}$ signaling is likely involved in both forward and reverse migration.

PI(3)K Is Necessary for Random Neutrophil Motility In Vivo

The finding that $\text{PI}(3,4,5)\text{P}_3\text{-PI}(3,4)\text{P}_2$ is polarized to the leading edge during both forward and reverse migration prompted us to determine if $\text{PI}(3)\text{K}$ is generally necessary for interstitial migration of neutrophils in vivo. Neutrophils migrate spontaneously and display apparent random motility in the mesenchymal tissues of the head at 2–3 dpf (Figure 3A; Movies S1 and S3A); this system was utilized to study random neutrophil motility within intact tissues. LY294002 treatment inhibited neutrophil random motility almost completely and induced morphological

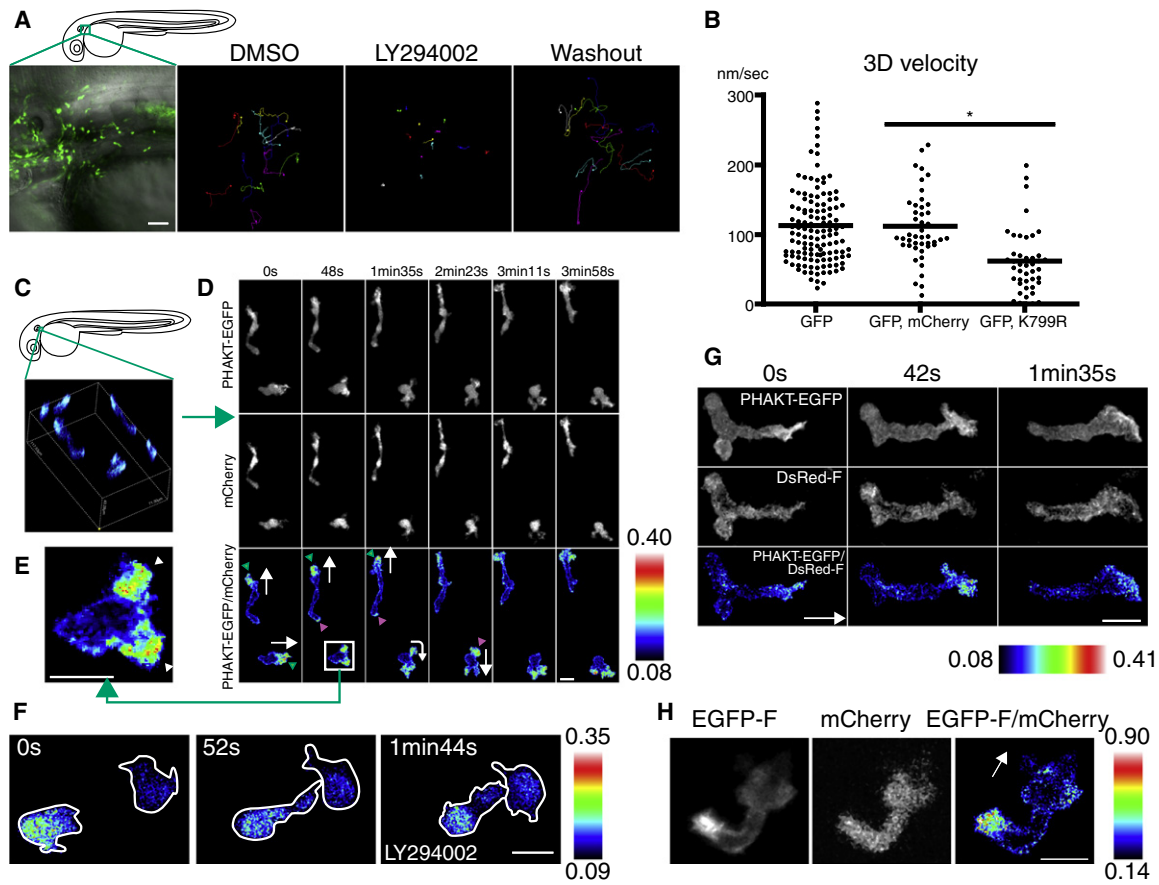


Figure 3. PI(3)K Is Critical for Neutrophil Motility and Is Active at the Leading Edge in the Mesenchymal Tissues of the Head

(A) Random migration of neutrophils is arrested by 65 μ M LY294002 and restored after washout of the drug. The lines indicate tracking of neutrophil motility (12 cells per condition) imaged for 30 min using *Tg(MPO:GFP)^{uvw}* (Movie S3A). Scale bar = 50 μ m.
 (B) PI(3)K γ K799R disturbs interstitial motility of neutrophils (Movie S3B, * $p < 0.001$, two-tailed unpaired t test; GFP: 128 neutrophils [40 movies], GFP, mCherry: 45 neutrophils [9 movies], GFP, K799R: 44 neutrophils [34 movies]).
 (C) Three-dimensional reconstruction of ratiometric image (PHAKT-EGFP/mCherry).
 (D) Time-lapse ratiometric imaging (PHAKT-EGFP/mCherry) of PI(3,4,5)P₃-PI(3,4)P₂ dynamics during random migration (Movie S4A). PI(3,4,5)P₃-PI(3,4)P₂ is mainly localized at the leading edge (green arrowheads) and occasionally at the tail (magenta arrow heads). White arrows indicate direction of migration. Scale bars in (D–H) = 10 μ m.
 (E) PI(3,4,5)P₃-PI(3,4)P₂ at the bifurcated pseudopod, indicated by arrowheads (Movie S4A).
 (F) Treatment with 65 μ M LY294002 inhibits the leading edge signal of PI(3,4,5)P₃-PI(3,4)P₂ and induces high ratiometric signals of PHAKT-EGFP/mCherry in the cell body of neutrophils (Movie S4C). Note the rounded tails and thin pseudopods induced by LY294002.
 (G) PI(3,4,5)P₃-PI(3,4)P₂ signal at the leading edge by ratiometric imaging of PHAKT-EGFP/farnesylated DsRed (DsRed-F) (Movie S4D). The white arrow indicates direction of migration.
 (H) Ratiometric imaging of EGFP-F/mCherry reveals periodic accumulation of membrane components at the tail (Movie S4E). The white arrow indicates direction of migration. Images are representative of three (A) and more than five (C–H) time-lapse movies from a minimum of three separate experiments.

changes including thin pseudopods and rounded tails (Figures 3A and 3F; Movie S3A). The impaired random motility and morphology defects were restored after washout of the drug (Figure 3A; Movie S3A). To exclude the possibility that the drug may alter neutrophil motility by affecting tissues surrounding the neutrophils, we expressed a dominant-negative construct of PI(3)K specifically in neutrophils. Although expression of $\Delta p85\alpha$, a deletion mutant of the adaptor subunit of class 1A PI(3)Ks, did not have apparent effects on neutrophil migration (data not shown), expression of K799R, a kinase-dead mutant of class 1B p110 γ (Takeda et al., 1999) induced morphology defects with thin pseudopods and rounded tails and impaired

neutrophil migration, suggesting that neutrophil PI(3)K γ is necessary for the interstitial migration of neutrophils in zebrafish (Figure 3B; Movie S3B). Consistent with this, the PI(3)K γ -specific inhibitor AS-605240 also impaired neutrophil motility (Movie S3C), and induced morphology defects similar to those observed with LY294002 and PI(3)K γ K799R.

We also imaged dynamics of PHAKT-EGFP/mCherry in the context of random migration, and found that PI(3,4,5)P₃-PI(3,4)P₂ is concentrated at bifurcated pseudopods of the leading edge, with the activity concentrated at dominant pseudopods and lost from retracted pseudopods (Figures 3C–3E; Movies S4A and S4B). We also noted occasional pulse signals

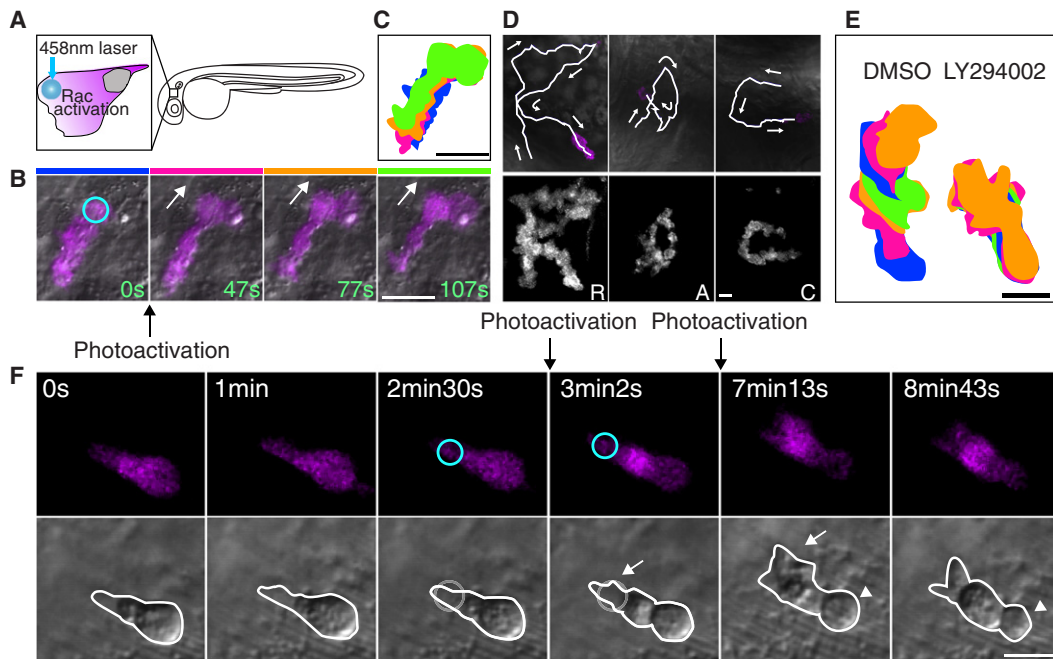


Figure 4. Photoactivation of Rac at the Leading Edge Can Rescue the Protrusion Defects but Not the Rounded Tail or Migration Defects Induced by PI(3)K Inhibition

(A) A schematic representation of photoactivation of Rac at the neutrophil leading edge in zebrafish. (B) Photoactivation of Rac at the leading edge induces protrusion and migration of a neutrophil in tissues (Movie S5). The circle indicates the position of Rac photoactivation. Scale bar = 20 μ m. (C) Overlaid images of (B) show directional migration induced by photoactivated Rac. Scale bar = 20 μ m. (D) Spelling by neutrophil trajectories guided through repetitive photoactivation of Rac at the leading edge (Movie S6). Scale bars in (D–F) = 10 μ m. (E) Overlaid images show that PI(3)K inhibition disturbs Rac photoactivation-induced migration. (The leading edge was activated for 20 s twice during 5 min imaging). (F) Photoactivation of Rac at the front (circles) can rescue the protrusion defect induced by PI(3)K inhibition (arrows), but not the rounded tail defect (arrowheads) (Movie S8). Images are representative of more than five time-lapse movies from experiments repeated on at least two separate dates.

of PI(3,4,5)P₃-PI(3,4)P₂ at the tail during random motility that were not apparent during directional migration (Figure 3D; Movies S4A and S4B). LY294002 treatment or PI(3)K γ K799R expression blocked signals of PI(3,4,5)P₃-PI(3,4)P₂ at the leading edge, indicating specificity of the probe to report PI(3)K activity (Figure 3F; Figures S3A and S3B and Movie S4C). Although PTEN phosphatase, which dephosphorylates PI(3,4,5)P₃-PI(3,4)P₂ at the 3 position, may modify the gradient of PI(3,4,5)P₃-PI(3,4)P₂, our results indicate that the polarized gradient of PI(3,4,5)P₃-PI(3,4)P₂ cannot be formed without PI(3)K activity. As a further control for the ratiometric analysis, we expressed farnesylated DsRed (DsRed-F) containing the farnesylation sequence of H-Ras, to provide a suitable membrane marker that cannot bind to negatively charged PI(3,4,5)P₃-PI(3,4)P₂ (Heo et al., 2006). Ratiometric imaging of this membrane-targeted DsRed-F and PHAKT-EGFP also yielded high signals at the leading edge (Figure 3G; Movie S4D). It is interesting to note that we did not observe the periodic high signals at the tail in the ratiometric imaging of PHAKT-EGFP/DsRed-F as seen with the combination of PHAKT-EGFP/mCherry during random motility. In fact, we found that the farnesylated membrane probe EGFP-F periodically accumulated at the tail (Figure 3H; Movie S4E). These findings indicate that PI(3,4,5)P₃-PI(3,4)P₂ is primarily localized to the leading edge but can also accumulate less frequently at the tail

as a membrane component. We found that this pulse of PI(3,4,5)P₃-PI(3,4)P₂ at the tail generally appears immediately after cell turning, presumably due to changes in membrane bulk at the uropod (Figure S3C and Movie S4B). Collectively, our results suggest that PI(3)K, specifically PI(3)K γ , is critical for neutrophil polarization and motility in intact tissues in vivo.

Photoactivation of Rac Is Sufficient to Direct Neutrophil Migration In Vivo, but Not the Migration of PI(3)K-Inhibited Cells

To elucidate how PI(3)K regulates neutrophil morphology and motility, we developed the tools to photoactivate a protein in specific cells of live zebrafish using a genetically encoded Rac1 GTPase which can be photoactivated reversibly and repeatedly by 458 nm light in tissue culture systems (Wu et al., 2009). The current dominant model proposes that PI(3)K regulates forward protrusion of the leading edge by activating Rac through a Rac GEF, such as DOCK (Nishikimi et al., 2009). We therefore examined whether localized activation of Rac at the cell front could rescue the morphology and migration defects induced by PI(3)K inhibition. First, we established a system to induce protrusion of the leading edge of neutrophils in live zebrafish by expressing the photoactivatable Rac specifically in neutrophils (Figure 4A). Single photoactivation of Rac at a given

cell edge generated protrusion from the stimulated edge quickly after stimulation, with protrusion lasting 2–3 min (Figure 4B; Movie S5), and induced directed migration (Figure 4C; Movie S5). Directed migration induced by photoactivation of Rac lasted only 2–3 min, presumably due to diffusion or dark recovery of photoactivated Rac (half-life of dark recovery is 43 s *in vitro* [Wu et al., 2009]). Stimulation with 458 nm light did not induce any obvious effects on morphology or migration of neutrophils expressing only mCherry (Figure S4A). Strikingly, repeated photoactivation of Rac at the leading edge was sufficient to direct neutrophil migration within tissues of zebrafish and to spell letters by guiding the trajectories of individual neutrophils (Figure 4D; Movie S6). This was performed by repeating photoactivation on a small circular area (diameter 2–5 μm) in the pseudopods at the leading edge. Interestingly, it was difficult to reverse neutrophil polarity and induce protrusion by performing photoactivation of Rac at the uropod in neutrophils migrating rapidly (data not shown), suggesting that the tail of polarized neutrophils are resistant to focal Rac-induced protrusion. This is consistent with previous reports suggesting that the uropod of polarized cells are resistant to becoming a new front (Devreotes and Janetopoulos, 2003; Xu et al., 2003). Guiding by photoactivation of Rac was also sufficient to impair neutrophil attraction to a wound, and was used to alter the direction of migration and to guide a neutrophil between the wound and the blood vessel (Figures S4B–S4D, and Movies S7A and S7B), suggesting that localized Rac activation can overcome endogenous chemotaxis signaling. Accordingly, photoactivation of Rac could also induce directed migration of relatively immotile neutrophils in the CHT (Figure S4E).

To determine if Rac activation was sufficient to rescue the migration defect of PI(3)K-inhibited cells, we induced polarized Rac activation at the leading edge in larvae exposed to PI(3)K inhibitors. Intriguingly, photoactivation of Rac at the leading edge of PI(3)K-inhibited neutrophils did not induce migration (Figure 4E). This was unexpected and contrary to the current dominant model that PI(3)K regulates migration through Rac activation at the leading edge. Further morphometric analysis revealed photoactivation of Rac at the leading edge can induce protrusion of the leading edge but cannot induce migration or a normal contracted tail (Figure 4F; Movie S8). We also confirmed similar results by using the PI(3)K γ -specific inhibitor AS-605240 (data not shown). These findings suggest that the tail and migration defect induced by PI(3)K inhibition is not just secondary to the protrusion defects.

Differential Regulation of Protrusion and Polarity by PI(3)K

The observation that protrusion of the leading edge can be rescued by photoactivation of Rac in PI(3)K-inhibited cells but that defects in tail morphology and migration cannot raised the question of how PI(3)K regulates the neutrophil uropod. We focused on the analysis of the cytoskeleton at the tail to elucidate how PI(3)K regulates the uropod. In typical cells over 2D surfaces, both dynamic (rapidly assembling and disassembling) and stable (slowly assembling and disassembling) populations of F-actin exist (Burkel et al., 2007). The dynamic F-actin is associated with transient force production and protrusion at the leading edge, while the more stable population is associated with more

sustained, myosin-dependent tail contraction. We used recently developed bioprobes for F-actin: calponin homology domain of utrophin fused to GFP, which detects a population of stable F-actin (Burkel et al., 2007) and Lifeact (17 amino acids of yeast Abp140) fused to Ruby, which detects all F-actin (Riedl et al., 2008). The biosensor for stable F-actin labels the tail of neutrophil-like cells *in vitro* under normal conditions (Cooper et al., 2008). By expressing the biosensors for stable F-actin and all F-actin, we revealed that neutrophils migrating *in vivo* have dynamic F-actin at the leading edge and stable F-actin predominantly at the tail (Figure 5A; Movies S9 and S10) and the lateral sides (Figure S5A). This is different from the blebbing-based motility employed by various types of cells in 3D environments but is consistent with the migration mode of dendritic cells in 3D (Insall and Machesky, 2009; Lammermann et al., 2008). Stable F-actin was also localized at the tail during migration toward or away from a wound and during photoactivation of Rac (Figure S5B and Movies S7B and S10), suggesting that the polarity of F-actin dynamics persists in all types of migration we examined. Interestingly, PI(3)K inhibition by LY294002 (Figures 5B and 5C; Movie S11A) or AS-605240 (Movie S11B) disturbed localization of stable F-actin at the tail and induced a more diffuse localization around the plasma membrane, suggesting that PI(3)K regulates the anteroposterior polarity of stable F-actin. Inhibition of Rho kinase or Myosin ATPase also inhibited normal accumulation of stable F-actin at the tail (Figure 5D; Movie S11C) while constitutively active Rho Q63L expression induced cell rounding and localization of stable F-actin all over the membrane (Figure 5E; Movie S12A). This strongly suggests that stable F-actin at the tail corresponds to the Rho-regulated actomyosin population in neutrophils *in vivo*. Rho inhibition by expression of a dominant-negative EGFP-RhoA T19N or EGFP-rGBD (RhoA binding domain of rhotekin fused to EGFP (Benink and Bement, 2005; Worthylake et al., 2001) induced rounding of the tail (Figure S5C, and Movies S12B and S12C). The similar phenotypes of stable F-actin mislocalization (Figures 5B–5D; Movies S11A, S11B, and S11C) and tail rounding (Figure 3F, Figure S5C, and Movies S4C, S12B, and S12C) induced by both inhibition of PI(3)K and Rho-Myosin signaling suggests that PI(3)K and Rho may function in a similar pathway to regulate the dynamics of F-actin and tail morphology. We also found that PI(3)K inhibition cannot relieve constitutively active Rho Q63L-mediated effects on cell rounding or localization of stable F-actin (Figure 5E; Movie S12A), suggesting that PI(3)K is not functioning downstream of Rho.

To address how PI(3)K regulates the polarization of stable F-actin, we determined whether localized Rac activation at the leading edge was sufficient to rescue targeting of the utrophin probe to the uropod in PI(3)K-inhibited cells. In controls, repetitive photoactivation of Rac induced protrusion of the leading edge with localization of stable F-actin at the tail (Figure 6A; Movies S7B and S13A). Unexpectedly, and in contrast to control cells, stable F-actin concentrated more at the leading edge than the tail after repetitive photoactivation of Rac at the leading edge of PI(3)K-inhibited cells (Figure 6B; Movie S13B). We observed similar results using AS-605240 (Figure S6 and Movie S13C). These findings indicate that PI(3)K is necessary for regulating anteroposterior polarity of F-actin dynamics in parallel with Rac activation at the leading edge. Accordingly, we found that in

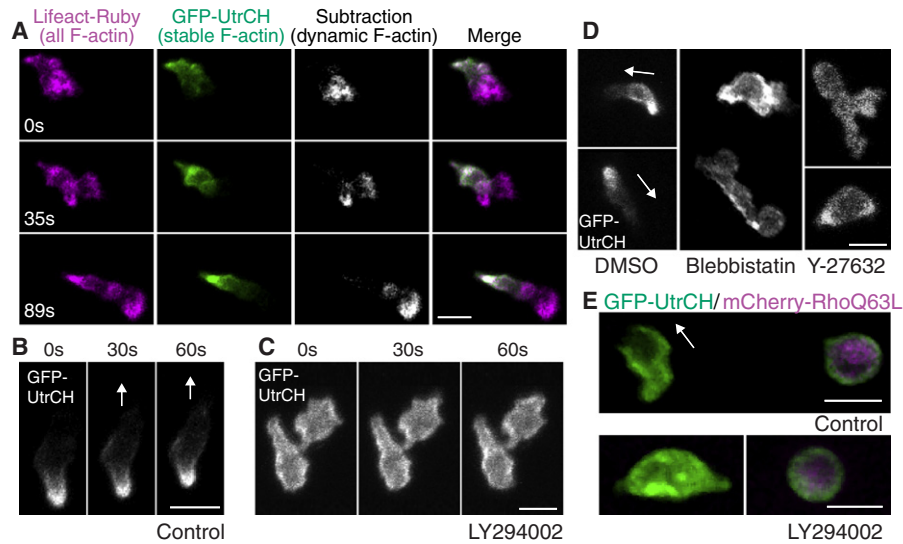


Figure 5. PI(3)K Regulates Anteroposterior Polarity of F-Actin Dynamics

(A) Stable F-actin (GFP-UtrCH) is localized at the tail while dynamic F-actin (Lifeact-Ruby subtracted by GFP-UtrCH) is localized at the front (Movie S9).

(B) In control, GFP-UtrCH labels the tail.

(C) PI(3)K inhibition by LY294002 disturbs tail localization of stable F-actin (Movie S11A).

(D) Myosin ATPase and Rho kinase inhibition disturbs tail localization of stable F-actin (Movie S11C).

(E) Constitutively active RhoQ63L induces cell rounding and localization of stable F-actin all over the membrane (top panel). PI(3)K inhibition does not relieve constitutively active Rho-mediated effects on cell rounding or localization of stable F-actin (lower panel) (Movie S12A). Images are representative of more than five time-lapse movies from experiments repeated on at least two separate dates.

Scale bars = 10 μ m.

the presence of PI(3)K inhibitor, after stopping photoactivation of Rac at the leading edge, protrusions induced by Rac activation often subsequently contracted and pushed the cell body to the opposite direction, becoming the tail (five out of seven movies, Figure S6, and Movie S13C). Taken together, the results indicate that PI(3)K activity at the leading edge is necessary to promote both “frontness” and “backness” signaling, and prevents the leading edge from becoming the tail by regulating the polarity of F-actin dynamics. Further, we examined whether positive feedback exists from Rac to PI(3)K, which has been suggested by previous studies in vitro (Srinivasan et al., 2003; Sun et al., 2004; Weiner et al., 2002). Photoactivation of Rac at the edge of an unpolarized neutrophil induced protrusion with polarized accumulation of PI(3,4,5)P₃-PI(3,4)P₂ (Figure 6C; Movie S14), suggesting that there is a positive feedback loop from Rac to PI(3,4,5)P₃-PI(3,4)P₂ production in neutrophils in vivo.

DISCUSSION

We uncoupled two roles for PI(3)K in regulating neutrophil motility: Rac-mediated protrusion of the leading edge, and polarization of F-actin dynamics that is separable from Rac activation. This two-tiered regulation of motility by PI(3)K can explain why PI(3)K is critical for neutrophil motility within complex tissues in vivo compared to its context-dependent roles in vitro (Andrew and Insall, 2007; Chen et al., 2007; Ferguson et al., 2007; Heit et al., 2008; Hoeller and Kay, 2007; Nishio et al., 2007). A previous report suggests that tail contraction is critical for migration in 3D environments by pushing the nucleus through narrow and constricted spaces (Lammermann et al., 2008). As another

example to support the importance of tail contraction for 3D migration, actomyosin-mediated tail contraction is not essential for motility of *D. discoideum* over 2D surfaces (De Lozanne and Spudich, 1987), but is indispensable for locomotion through 3D matrices that offer resistance (Laevsky and Knecht, 2003). The idea that PI(3)K is important for actomyosin-mediated tail contraction is consistent with the previous report that PI(3)K regulates extravasation from the blood vessel (Liu et al., 2007) because neutrophils need to be contracted to go through a narrow space between endothelial cells. Although we suggest that PI(3)K-mediated anteroposterior polarity of F-actin dynamics is not through Rac activation at the leading edge, several lines of evidence from in vitro studies suggest that Rac regulates Rho activity or actomyosin contraction (Pestonjasp et al., 2006; Wu et al., 2009). It is intriguing to speculate that Rac may regulate uropod events via PI(3)K activation, through the feedback loop from Rac to PI(3,4,5)P₃-PI(3,4)P₂ polarity that has been reported in vitro (Srinivasan et al., 2003; Sun et al., 2004; Weiner et al., 2002) and was demonstrated in vivo in this study.

It remains elusive how the PI(3,4,5)P₃-PI(3,4)P₂ gradient regulates polarity of F-actin dynamics, but our data suggest that inhibition of PI(3)K and Rho-ROCK-Myosin pathway leads to similar phenotypes: a rounded tail and loss of stable F-actin polarity. Although spatiotemporal regulation is not clear, PI(3)K was previously demonstrated to suppress basal activity of Rho (Papakonstanti et al., 2007; Van Keymeulen et al., 2006) or to regulate ROCK in vitro (Niggli, 2000). Together with our data, this raises the possibility that PI(3)K, which is mainly active at the leading edge, regulates Rho-ROCK-Myosin-mediated

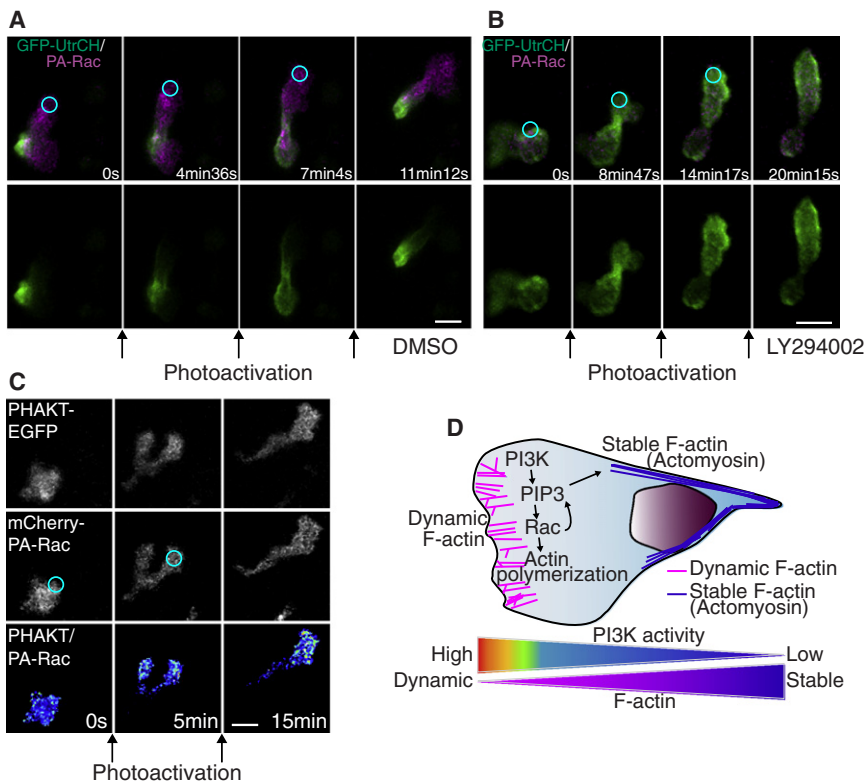


Figure 6. PI(3)K Regulates Anteroposterior Polarity of F-Actin Dynamics in a Pathway That Is Separable from Rac-Mediated Protrusion

(A) In control, photoactivation of Rac at the leading edge induces protrusion at the leading edge with GFP-UtrCH (stable F-actin) localized at the tail (Movie S13A).

(B) Photoactivation of Rac with PI(3)K inhibition induces protrusion with GFP-UtrCH (stable F-actin) localized at the leading edge, indicating reverse polarity of F-actin dynamics (Movie S13B).

(C) Protrusion induced by photoactivation of Rac induces PHAKT-EGFP accumulation at the leading edge, suggesting a positive feedback from Rac to PI(3,4,5)P₃-PI(3,4)P₂ gradient (Movie S14).

(D) A schematic representation of two-tiered PI(3)K-mediated regulation of cell motility: PI(3)K promotes Rac-mediated actin polymerization at the leading edge while generating anteroposterior polarity of F-actin dynamics. Images are representative of more than five time-lapse movies from experiments repeated on at least two separate dates.

Scale bars = 10 μm.

uropod contraction. A possible hypothesis is that PI(3)K might inhibit Rho activity at the leading edge through regulating, for example, a Rho GAP and creating gradients of Rho activity from the front to the back. Among Rho GAPs, Arap3, which was screened out as a binding protein to PI(3,4,5)P₃, is a candidate to mediate PI(3)K-dependent Rho regulation from the front to the back (Krugmann et al., 2002). As another possibility, PI(3,4,5)P₃-PI(3,4)P₂ pulse which occasionally appears at the tail as a membrane component (Figure 3D) might regulate uropod events directly. Although we cannot rule out this possibility, a role of PI(3,4,5)P₃-PI(3,4)P₂ as an instructive cue at the tail is unlikely because the pulse of PI(3,4,5)P₃-PI(3,4)P₂ at the tail is much less frequent than PI(3,4,5)P₃-PI(3,4)P₂ at the front or stable F-actin at the tail. Thus, we speculate that PI(3,4,5)P₃-PI(3,4)P₂ at the tail would have a permissive role together with other instructive cues at the tail if there is a specific function. Alternatively PI(3)K might regulate polarity of F-actin dynamics through Hem-1 (Weiner et al., 2006) or Pak (Chung et al., 2001), which were suggested to regulate Rho and/or myosin-mediated tail contraction. It is also possible that PI(3)K might induce a gradient of F-actin dynamics through cofilin activator slingshot, which is activated downstream of PI(3)K in tissue culture systems (Nishita et al., 2004). Finally, the defects in uropod morphology and F-actin dynamics in PI(3)K-inhibited cells might also be due to altered adhesion at the leading edge. Although we cannot rule out this hypothesis, the scenario of adhesion-mediated consolidation at the front needs to be reconciled with the recent report that leukocytes migrate in the absence of specific adhesive interactions within 3D environments (Lammermann et al., 2008).

Here, for the first time, we have visualized the dynamics of PI(3)K products PI(3,4,5)P₃-PI(3,4)P₂ during neutrophil migration in intact tissues in vivo. We have shown that PI(3)K is critical for neutrophil polarity and motility in vivo. Cell migration could be directed in vivo with precise spatiotemporal control using light-mediated activation of a novel genetically encoded photoactivatable Rac. This enabled us to demonstrate that Rac activation at the leading edge was sufficient to rescue membrane protrusion but not directed cell migration or polarity of F-actin dynamics in PI(3)K-inhibited cells. With the majority of current data supporting a model that PI(3)K regulates migration by promoting Rac-mediated leading edge formation, our findings that PI(3)K regulates gradients of F-actin dynamics in a pathway that is separable from Rac-mediated protrusion suggest a new paradigm of two-tiered regulation of cell motility by PI(3)K: PI(3)K promotes Rac-mediated actin polymerization at the leading edge while generating anteroposterior polarity of F-actin dynamics (Figure 6D).

EXPERIMENTAL PROCEDURES

DNA Expression Vectors, RNA Synthesis, and Injection

All DNA expression vectors contain the zMPO promoter for neutrophil expression (Mathias et al., 2006), minimal Tol2 elements for efficient integration (Urasaki et al., 2006), and an SV40 polyadenylation sequence (Clontech Laboratories, Inc). A construct containing full-length Tol2 transposon arms was kindly provided by M. Nonet and was used to create the minimal Tol2 elements as described previously (Urasaki et al., 2006). Constructs which have each of the following sequences in this backbone vector were constructed: PHAKT-EGFP (PH domain of AKT fused to EGFP, the original plasmid is a generous gift from T. Balla), mCherry (the original plasmid is a generous gift from

R. Tsien), DsRed-F (DsRed with the farnesylation sequence of H-Ras at the C terminus, Clontech Laboratories, INC), EGFP-F (EGFP with the farnesylation sequence of H-Ras at the C terminus), EGFP-UtrCH (calponin homology domain of utrophin fused to EGFP, the original plasmid is a generous gift from W. Bement) (Burkel et al., 2007), EGFP-rGBD (RhoA binding domain of rhotekin fused to EGFP, the original plasmid is a generous gift from W. Bement) (Benink and Bement, 2005), mCherry-PA-Rac1 (Wu et al., 2009), mCherry-RhoA Q63L or EGFP-RhoA T19N (the original plasmids are generous gifts from G. Bokoch), and Lifeact-Ruby (the original plasmid is a generous gift from M. Sixt). We also made constructs in which bovine $\Delta p85\alpha$ (a generous gift from M. Vicente-Manzanares) and human K799R p110 γ (generated by PCR mutagenesis of the IMAGE clone 5749986 [ATCC]) were fused to mCherry respectively by 2A-peptide (the original plasmid is a generous gift from E. Provost), which drives separate expression of two proteins (Provost et al., 2007). Transposase mRNA was synthesized from pCS-TP by in vitro transcription (Invitrogen). For injection of a single construct, 0.5 nL of solution containing 25 ng/ μ L DNA plasmid and 35 ng/ μ L Transposase mRNA was injected into the cytoplasm of one-cell stage embryos, as described previously (Fisher et al., 2006). For injection of two constructs, 0.5 nL of solution containing 12.5 ng/ μ L of each construct and 35 ng/ μ L Transposase mRNA was injected into the cytoplasm of one-cell stage embryos. DNA plasmids with the Tol2-zMPO backbone were injected and expressed transiently as described in the Supplemental Information.

Live Imaging and Laser Wounding

Embryos at 2–3 days post fertilization (dpf) were settled on a glass-bottom dish for live imaging. For imaging longer than 1 hr, embryos were embedded in 1% low-melting point agarose. Time-lapse fluorescence images were acquired with a confocal microscope (FluoView FV1000, Olympus) using a NA 0.75/20 \times objective or a NA 1.10/60 \times water immersion objective lens. Each fluorescence channel and the DIC images were acquired by sequential line scanning. Z-series were acquired using 260–600 μ m pinhole and 2–10 μ m step sizes. Z series images were stacked or 3D-reconstructed by the FluoView FV1000 software (Olympus). To make overlay images of DIC and fluorescence or ratio-metric pictures, Z stacked fluorescence or ratio-metric images were overlaid onto a single DIC plane. Laser wounding was performed by focusing the 405 nm diode laser with the maximal power into a small circular area (diameter 1 μ m) for 30–60 s. An autofluorescent pigment was targeted by the laser for wounding in the caudal hematopoietic tissue (CHT). Where indicated, embryos were pretreated with 65 μ M LY294002 (Calbiochem), 100 μ M Blebbistatin (Calbiochem), 10 μ M AS-605240 (Sigma Aldrich) for 1 hr or 500 μ M Y-27632 (Calbiochem) for 2–3 hr, then images were taken with drugs in E3.

Photoactivation of mCherry-PA-Rac1

Embryos injected with Tol2-MPO-mCherry-PA-Rac1-polyA or *Tg(MPO:mCherry-PA-Rac1)^{luc}* were imaged at 2–3 dpf. Because high expression of this protein leads to leaky activation of Rac without stimulation, we carefully selected cells which had a normal polarized morphology with moderate expression of mCherry-PA-Rac1. For efficiency of activation by light, we only targeted neutrophils on the surface of the head, yolk, midbody, or fin. To induce cell protrusion, 458 nm laser was focused into a small circular area (diameter 2–5 μ m) for 20–30 s with 3% power 10.0 μ s/pixel (tornado function) with a confocal microscope (FluoView FV1000, Olympus) using a NA 0.75/20 \times objective (Wu et al., 2009). To induce directional migration or guide neutrophils, this procedure was repeated every 2–3 min at the leading edge of neutrophils.

Tail Fin Wounding and Sudan-Black Staining of Neutrophils

Embryos pretreated with DMSO, LY294002 (32.5–65 μ M), or AS-605240 (2.5–10 μ M) for 1 hr at 3 dpf or morphants at 2 dpf were anesthetized by 0.2 mg/mL Tricaine, and wounded at the tail fin with a needle. Sudan-black staining of neutrophils was performed as described previously (Le Guyader et al., 2008; Levraud et al., 2008). Embryos were fixed 1 hr after wounding in 4% formaldehyde in PBS for 1.5 hr at room temperature, rinsed in PBS, incubated in 0.03% Sudan Black, followed by extensive washing in 70% ethanol. After rehydration to PBST (0.1% Tween-20), pigments were removed by incubation in 1% H₂O₂, 1% KOH solution. Embryos were observed using a Nikon SMZ-1500 zoom microscope (Nikon).

SUPPLEMENTAL INFORMATION

Supplemental Information includes six figures, fourteen movies, and Supplemental Experimental Procedures and can be found with this article online at doi:10.1016/j.devcel.2009.11.015.

ACKNOWLEDGMENTS

We thank J.R. Mathias for technical assistance and reviewing the original manuscript; M.E. Dodd for construction of the Tol2 backbone vector and reviewing the manuscript; A.F. Bent, K.T. Chan, K.B. Walters, A.J. Wiemer, W.T.N. Simonson, and S.A. Wernimont for critical reading of the manuscript; P.-Y Lam for assistance of revision; E. Zeiss (Leeds) for help with the confocal microscope; M. Nonet, T. Balla, R. Tsien, E. Provost, W. Bement, M. Vicente-Manzanares, E. Provost, G. Bokoch, and M. Sixt for generous gift of plasmids. This work was supported by National Institutes of Health Grants GM074827 (A.H.), T32ES007015 (P.J.C.), GM057464 (K.M.H.), GM64346 (K.M.H.), and the American Heart Association (Y.W.).

Received: August 9, 2009

Revised: October 29, 2009

Accepted: November 23, 2009

Published: February 15, 2010

REFERENCES

- Andrew, N., and Insall, R.H. (2007). Chemotaxis in shallow gradients is mediated independently of PtdIns 3-kinase by biased choices between random protrusions. *Nat. Cell Biol.* 9, 193–200.
- Arriemerlou, C., and Meyer, T. (2005). A local coupling model and compass parameter for eukaryotic chemotaxis. *Dev. Cell* 8, 215–227.
- Barberis, L., and Hirsch, E. (2008). Targeting phosphoinositide 3-kinase γ to fight inflammation and more. *Thromb. Haemost.* 99, 279–285.
- Benink, H.A., and Bement, W.M. (2005). Concentric zones of active RhoA and Cdc42 around single cell wounds. *J. Cell Biol.* 168, 429–439.
- Burkel, B.M., von Dassow, G., and Bement, W.M. (2007). Versatile fluorescent probes for actin filaments based on the actin-binding domain of utrophin. *Cell Motil. Cytoskeleton* 64, 822–832.
- Camps, M., Ruckle, T., Ji, H., Ardisson, V., Rintelen, F., Shaw, J., Ferrandi, C., Chabert, C., Gillieron, C., Francon, B., et al. (2005). Blockade of PI3K γ suppresses joint inflammation and damage in mouse models of rheumatoid arthritis. *Nat. Med.* 11, 936–943.
- Chen, L., Iijima, M., Tang, M., Landree, M.A., Huang, Y.E., Xiong, Y., Iglesias, P.A., and Devreotes, P.N. (2007). PLA2 and PI3K/Pten pathways act in parallel to mediate chemotaxis. *Dev. Cell* 12, 603–614.
- Chung, C.Y., Potikyan, G., and Firtel, R.A. (2001). Control of cell polarity and chemotaxis by Akt/PKB and PI3 kinase through the regulation of PAKa. *Mol. Cell* 7, 937–947.
- Cooper, K.M., Bennin, D.A., and Huttenlocher, A. (2008). The PCH family member proline-serine-threonine phosphatase-interacting protein 1 targets to the leukocyte uropod and regulates directed cell migration. *Mol. Biol. Cell* 19, 3180–3191.
- Cukierman, E., Pankov, R., Stevens, D.R., and Yamada, K.M. (2001). Taking cell-matrix adhesions to the third dimension. *Science* 294, 1708–1712.
- Cvejic, A., Hall, C., Bak-Maier, M., Flores, M.V., Crosier, P., Redd, M.J., and Martin, P. (2008). Analysis of WASp function during the wound inflammatory response—live-imaging studies in zebrafish larvae. *J. Cell Sci.* 121, 3196–3206.
- De Lozanne, A., and Spudich, J.A. (1987). Disruption of the *Dictyostelium* myosin heavy chain gene by homologous recombination. *Science* 236, 1086–1091.
- Devreotes, P., and Janetopoulos, C. (2003). Eukaryotic chemotaxis: distinctions between directional sensing and polarization. *J. Biol. Chem.* 278, 20445–20448.
- Dumstrei, K., Mennecke, R., and Raz, E. (2004). Signaling pathways controlling primordial germ cell migration in zebrafish. *J. Cell Sci.* 117, 4787–4795.

- Ferguson, G.J., Milne, L., Kulkarni, S., Sasaki, T., Walker, S., Andrews, S., Crabbe, T., Finan, P., Jones, G., Jackson, S., et al. (2007). PI(3)K γ has an important context-dependent role in neutrophil chemokinesis. *Nat. Cell Biol.* **9**, 86–91.
- Fisher, S., Grice, E.A., Vinton, R.M., Bessling, S.L., Urasaki, A., Kawakami, K., and McCallion, A.S. (2006). Evaluating the biological relevance of putative enhancers using Tol2 transposon-mediated transgenesis in zebrafish. *Nat. Protoc.* **1**, 1297–1305.
- Grabher, C., Cliffe, A., Miura, K., Hayflick, J., Pepperkok, R., Rorth, P., and Wittbrodt, J. (2007). Birth and life of tissue macrophages and their migration in embryogenesis and inflammation in medaka. *J. Leukoc. Biol.* **81**, 263–271.
- Hawkins, P.T., and Stephens, L.R. (2007). PI3K γ is a key regulator of inflammatory responses and cardiovascular homeostasis. *Science* **318**, 64–66.
- Heit, B., Robbins, S.M., Downey, C.M., Guan, Z., Colarusso, P., Miller, B.J., Jirik, F.R., and Kubes, P. (2008). PTEN functions to ‘prioritize’ chemotactic cues and prevent ‘distraction’ in migrating neutrophils. *Nat. Immunol.* **9**, 743–752.
- Heo, W.D., Inoue, T., Park, W.S., Kim, M.L., Park, B.O., Wandless, T.J., and Meyer, T. (2006). PI(3,4,5)P3 and PI(4,5)P2 lipids target proteins with polybasic clusters to the plasma membrane. *Science* **314**, 1458–1461.
- Hirsch, E., Katanaev, V.L., Garlanda, C., Azzolino, O., Pirota, L., Silengo, L., Sozzani, S., Mantovani, A., Altruda, F., and Wymann, M.P. (2000). Central role for G protein-coupled phosphoinositide 3-kinase γ in inflammation. *Science* **287**, 1049–1053.
- Hoeller, O., and Kay, R.R. (2007). Chemotaxis in the absence of PIP3 gradients. *Curr. Biol.* **17**, 813–817.
- Insell, R.H., and Machesky, L.M. (2009). Actin dynamics at the leading edge: from simple machinery to complex networks. *Dev. Cell* **17**, 310–322.
- Janetopoulos, C., and Firtel, R.A. (2008). Directional sensing during chemotaxis. *FEBS Lett.* **582**, 2075–2085.
- Kay, R.R., Langridge, P., Traynor, D., and Hoeller, O. (2008). Changing directions in the study of chemotaxis. *Nat. Rev. Mol. Cell Biol.* **9**, 455–463.
- Krugmann, S., Anderson, K.E., Ridley, S.H., Rizzo, N., McGregor, A., Coadwell, J., Davidson, K., Eguinoa, A., Ellson, C.D., Lipp, P., et al. (2002). Identification of ARAP3, a novel PI3K effector regulating both Arf and Rho GTPases, by selective capture on phosphoinositide affinity matrices. *Mol. Cell* **9**, 95–108.
- Laevsky, G., and Knecht, D.A. (2003). Cross-linking of actin filaments by myosin II is a major contributor to cortical integrity and cell motility in restrictive environments. *J. Cell Sci.* **116**, 3761–3770.
- Lammermann, T., Bader, B.L., Monkley, S.J., Worbs, T., Wedlich-Soldner, R., Hirsch, K., Keller, M., Forster, R., Critchley, D.R., Fassler, R., et al. (2008). Rapid leukocyte migration by integrin-independent flowing and squeezing. *Nature* **453**, 51–55.
- Le Guyader, D., Redd, M.J., Colucci-Guyon, E., Murayama, E., Kissa, K., Briolat, V., Mordelet, E., Zapata, A., Shinomiya, H., and Herbomel, P. (2008). Origins and unconventional behavior of neutrophils in developing zebrafish. *Blood* **111**, 132–141.
- Levrud, J.P., Colucci-Guyon, E., Redd, M.J., Lutfalla, G., and Herbomel, P. (2008). In vivo analysis of zebrafish innate immunity. *Methods Mol. Biol.* **415**, 337–363.
- Li, Z., Jiang, H., Xie, W., Zhang, Z., Smrcka, A.V., and Wu, D. (2000). Roles of PLC- β 2 and - β 3 and PI3K γ in chemoattractant-mediated signal transduction. *Science* **287**, 1046–1049.
- Liu, L., Puri, K.D., Penninger, J.M., and Kubes, P. (2007). Leukocyte PI3K γ and PI3K δ have temporally distinct roles for leukocyte recruitment in vivo. *Blood* **110**, 1191–1198.
- Mathias, J.R., Perrin, B.J., Liu, T.X., Kanki, J., Look, A.T., and Huttenlocher, A. (2006). Resolution of inflammation by retrograde chemotaxis of neutrophils in transgenic zebrafish. *J. Leukoc. Biol.* **80**, 1281–1288.
- Mizoguchi, T., Verkade, H., Heath, J.K., Kuroiwa, A., and Kikuchi, Y. (2008). Sdf1/Cxcr4 signaling controls the dorsal migration of endodermal cells during zebrafish gastrulation. *Development* **135**, 2521–2529.
- Murayama, E., Kissa, K., Zapata, A., Mordelet, E., Briolat, V., Lin, H.F., Handin, R.I., and Herbomel, P. (2006). Tracing hematopoietic precursor migration to successive hematopoietic organs during zebrafish development. *Immunity* **25**, 963–975.
- Niethammer, P., Grabher, C., Look, A.T., and Mitchison, T.J. (2009). A tissue-scale gradient of hydrogen peroxide mediates rapid wound detection in zebrafish. *Nature* **459**, 996–999.
- Niggli, V. (2000). A membrane-permeant ester of phosphatidylinositol 3,4,5-trisphosphate (PIP(3)) is an activator of human neutrophil migration. *FEBS Lett.* **473**, 217–221.
- Niggli, V., and Keller, H. (1997). The phosphatidylinositol 3-kinase inhibitor wortmannin markedly reduces chemotactic peptide-induced locomotion and increases in cytoskeletal actin in human neutrophils. *Eur. J. Pharmacol.* **335**, 43–52.
- Nishikimi, A., Fukuhara, H., Su, W., Hongu, T., Takasuga, S., Mihara, H., Cao, Q., Sanematsu, F., Kanai, M., Hasegawa, H., et al. (2009). Sequential regulation of DOCK2 dynamics by two phospholipids during neutrophil chemotaxis. *Science* **324**, 384–387.
- Nishio, M., Watanabe, K., Sasaki, J., Taya, C., Takasuga, S., Iizuka, R., Balla, T., Yamazaki, M., Watanabe, H., Itoh, R., et al. (2007). Control of cell polarity and motility by the PtdIns(3,4,5)P3 phosphatase SHIP1. *Nat. Cell Biol.* **9**, 36–44.
- Nishita, M., Wang, Y., Tomizawa, C., Suzuki, A., Niwa, R., Uemura, T., and Mizuno, K. (2004). Phosphoinositide 3-kinase-mediated activation of cofilin phosphatase Slingshot and its role for insulin-induced membrane protrusion. *J. Biol. Chem.* **279**, 7193–7198.
- Nombela-Arrieta, C., Lacalle, R.A., Montoya, M.C., Kunisaki, Y., Megias, D., Marques, M., Carrera, A.C., Manes, S., Fukui, Y., Martinez, A.C., et al. (2004). Differential requirements for DOCK2 and phosphoinositide-3-kinase γ during T and B lymphocyte homing. *Immunity* **21**, 429–441.
- Papakonstanti, E.A., Ridley, A.J., and Vanhaesebroeck, B. (2007). The p110 δ isoform of PI 3-kinase negatively controls RhoA and PTEN. *EMBO J.* **26**, 3050–3061.
- Parent, C.A., Blacklock, B.J., Froehlich, W.M., Murphy, D.B., and Devreotes, P.N. (1998). G protein signaling events are activated at the leading edge of chemotactic cells. *Cell* **95**, 81–91.
- Pestonjamas, K.N., Forster, C., Sun, C., Gardiner, E.M., Bohl, B., Weiner, O., Bokoch, G.M., and Glogauer, M. (2006). Rac1 links leading edge and uropod events through Rho and myosin activation during chemotaxis. *Blood* **108**, 2814–2820.
- Provost, E., Rhee, J., and Leach, S.D. (2007). Viral 2A peptides allow expression of multiple proteins from a single ORF in transgenic zebrafish embryos. *Genesis* **45**, 625–629.
- Reicha, E.C., and Parent, C.A. (2008). Steering in quadruplet: the complex signaling pathways directing chemotaxis. *Sci. Signal.* **1**, pe26.
- Riedl, J., Crevenna, A.H., Kessenbrock, K., Yu, J.H., Neukirchen, D., Bista, M., Bradke, F., Jenne, D., Holak, T.A., Werb, Z., et al. (2008). Lifeact: a versatile marker to visualize F-actin. *Nat. Methods* **5**, 605–607.
- Sasaki, T., Irie-Sasaki, J., Jones, R.G., Oliveira-dos-Santos, A.J., Stanford, W.L., Bolon, B., Wakeham, A., Itie, A., Bouchard, D., Kozieradzki, I., et al. (2000). Function of PI3K γ in thymocyte development, T cell activation, and neutrophil migration. *Science* **287**, 1040–1046.
- Servant, G., Weiner, O.D., Herzmark, P., Balla, T., Sedat, J.W., and Bourne, H.R. (2000). Polarization of chemoattractant receptor signaling during neutrophil chemotaxis. *Science* **287**, 1037–1040.
- Srinivasan, S., Wang, F., Glavas, S., Ott, A., Hofmann, F., Aktories, K., Kalman, D., and Bourne, H.R. (2003). Rac and Cdc42 play distinct roles in regulating PI(3,4,5)P3 and polarity during neutrophil chemotaxis. *J. Cell Biol.* **160**, 375–385.
- Stephens, L., Milne, L., and Hawkins, P. (2008). Moving towards a better understanding of chemotaxis. *Curr. Biol.* **18**, R485–R494.
- Sun, C.X., Downey, G.P., Zhu, F., Koh, A.L., Thang, H., and Glogauer, M. (2004). Rac1 is the small GTPase responsible for regulating the neutrophil chemotaxis compass. *Blood* **104**, 3758–3765.
- Takeda, H., Matozaki, T., Takada, T., Noguchi, T., Yamao, T., Tsuda, M., Ochi, F., Fukunaga, K., Inagaki, K., and Kasuga, M. (1999). PI 3-kinase γ and protein

- kinase C- ζ mediate RAS-independent activation of MAP kinase by a Gi protein-coupled receptor. *EMBO J.* 18, 386–395.
- Trede, N.S., Langenau, D.M., Traver, D., Look, A.T., and Zon, L.I. (2004). The use of zebrafish to understand immunity. *Immunity* 20, 367–379.
- Urasaki, A., Morvan, G., and Kawakami, K. (2006). Functional dissection of the Tol2 transposable element identified the minimal cis-sequence and a highly repetitive sequence in the subterminal region essential for transposition. *Genetics* 174, 639–649.
- Van Haastert, P.J., and Veltman, D.M. (2007). Chemotaxis: navigating by multiple signaling pathways. *Sci. STKE* 2007, pe40.
- Van Keymeulen, A., Wong, K., Knight, Z.A., Govaerts, C., Hahn, K.M., Shokat, K.M., and Bourne, H.R. (2006). To stabilize neutrophil polarity, PIP3 and Cdc42 augment RhoA activity at the back as well as signals at the front. *J. Cell Biol.* 174, 437–445.
- Vanhaesebroeck, B., Ali, K., Bilancio, A., Geering, B., and Foukas, L.C. (2005). Signalling by PI3K isoforms: insights from gene-targeted mice. *Trends Biochem. Sci.* 30, 194–204.
- Weiner, O.D., Neilsen, P.O., Prestwich, G.D., Kirschner, M.W., Cantley, L.C., and Bourne, H.R. (2002). A PtdInsP(3)- and Rho GTPase-mediated positive feedback loop regulates neutrophil polarity. *Nat. Cell Biol.* 4, 509–513.
- Weiner, O.D., Rentel, M.C., Ott, A., Brown, G.E., Jedrychowski, M., Yaffe, M.B., Gygi, S.P., Cantley, L.C., Bourne, H.R., and Kirschner, M.W. (2006). Hem-1 complexes are essential for Rac activation, actin polymerization, and myosin regulation during neutrophil chemotaxis. *PLoS Biol.* 4, e38.
- Worthylake, R.A., Lemoine, S., Watson, J.M., and Burridge, K. (2001). RhoA is required for monocyte tail retraction during transendothelial migration. *J. Cell Biol.* 154, 147–160.
- Wu, Y.I., Frey, D., Lungu, O.I., Jaehrig, A., Schlichting, I., Kuhlman, B., and Hahn, K.M. (2009). A genetically encoded photoactivatable Rac controls the motility of living cells. *Nature* 461, 104–108.
- Xu, J., Wang, F., Van Keymeulen, A., Herzmark, P., Straight, A., Kelly, K., Takuwa, Y., Sugimoto, N., Mitchison, T., and Bourne, H.R. (2003). Divergent signals and cytoskeletal assemblies regulate self-organizing polarity in neutrophils. *Cell* 114, 201–214.